Supporting Information

Mechanisms of Enhanced Sulfur Tolerance on Samarium (Sm)-doped Cerium Oxide (CeO_2) from First Principles

Dong-Hee Lim[1),2)], Hee Su Kim[1)], Sung Pil Yoon[1)], Jonghee Han[1)], Chang Won Yoon[1)], Sun Hee Choi[1)], Suk Woo Nam[1)], and Hyung Chul Ham[1),*]

[1)] Fuel Cell Research Center, Korea Institute of Science and Technology (KIST), Hwarangno 14-gil 5, Seongbuk-gu, Seoul 136-791, Republic of Korea

[2)] Department of Environmental Engineering, Chungbuk National University 52 Naesudong-ro, Heungdeok-gu, Cheongju, Chungbuk 361-763, Republic of Korea

*Corresponding Author: Hyung Chul Ham

Email: hchahm@kist.re.kr

Phone: +82-2-958-5889, Fax: +82-2-958-5199

1. H_2S decomposition and SO_2 formation pathways

The activation energies for H_2S decomposition and SO_2 formation were determined along the examined pathways as shown in Figure S1 (note that H atoms were not taken into account in the activation energy calculations of SO_2 formation reaction).

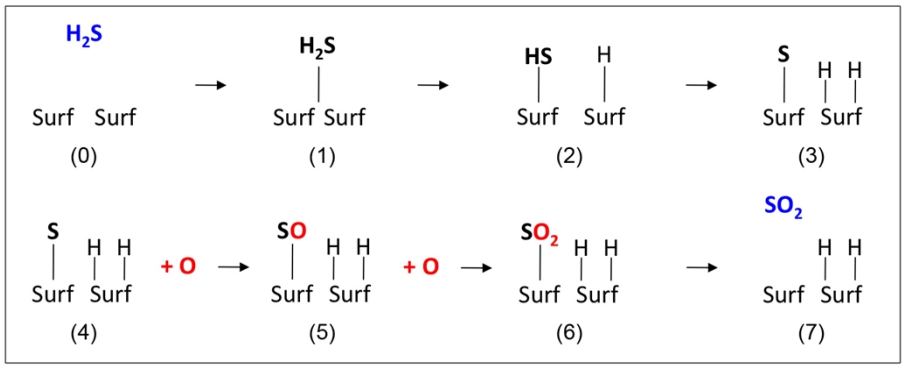

Figure S1. Schematic diagrams of H_2S decomposition and SO_2 formation on stoichiometric CeO_2 and Sm-doped CeO_2.

An overall reaction pathway from H_2S adsorption to SO_2 desorption was examined by calculating total energy change (ΔE) between two adsorbed intermediates; for example, $\Delta E_{H2S*-HS*} = E_{HS*} + E_{H*} - E_{H2S*} - E_{*}$, where $\Delta E_{H2S*-HS*}$ is ΔE between H_2S^* and HS^*, E is the total energy of a surface with adsorbed species, subscripts are adsorbed species, and E_* is the total energy of a clean surface.

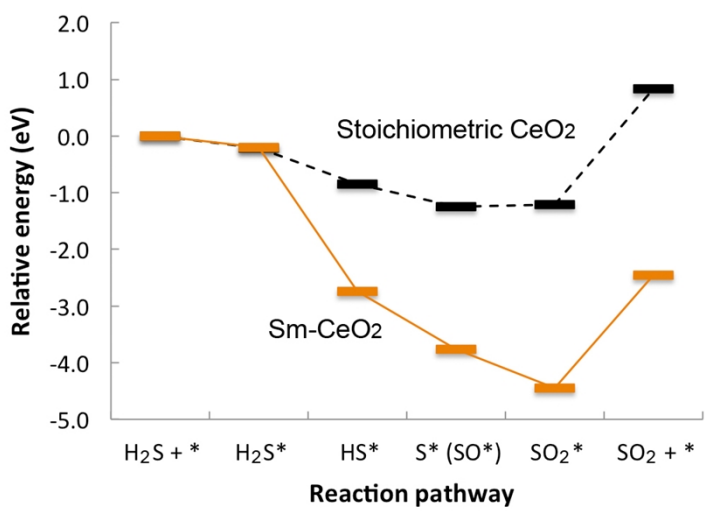

Figure S2. The overall reaction pathways of H_2S decomposition and SO_2 formation on stoichiometric CeO_2 (dashed lines) and Sm-doped CeO_2 (solid lines). * and S^* (SO^*) indicate a clean surface and adsorbed sulfur on lattice oxygen, respectively.

2. Adsorption configurations of $S^* + H^* + H^*$ on stoichiometric CeO_2

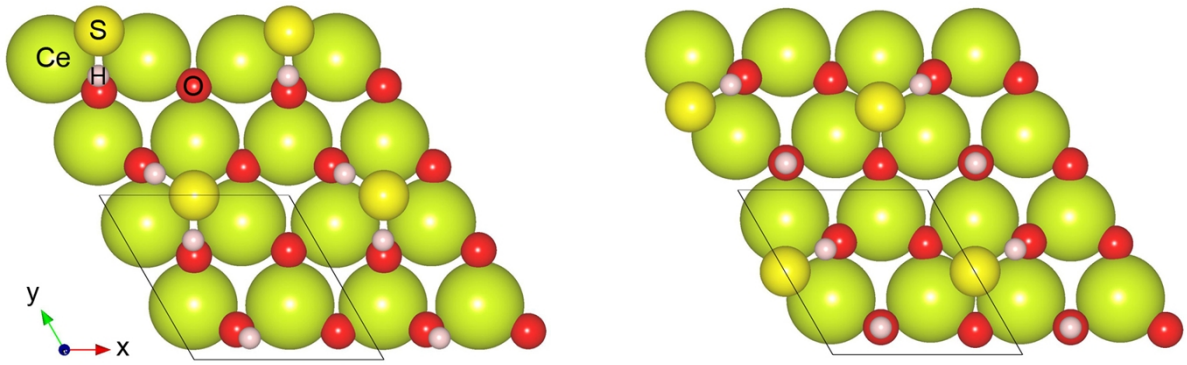

(a) 0.15 eV (b) 0.19 eV

Figure S3. Adsorption configurations of $S^* + H^* + H^*$ at hollow sties of stoichiometric CeO_2. (a) and (b) energies indicate relative energies of each configuration compared to the total energy of $S^* + H^* + H^*$ on CeO_2 where sulfur is located at the top site of Ce as shown in Figure 2 Case(I) of the main paper.

3. Adsorption of H_2S, HS, and S species

Table S1. Adsorption energies (E_{ad}) of H_2S, HS, and S species on the stoichiometric CeO_2 and Sm-doped CeO_2 surfaces depending on adsorption sites. H_2S adsorption calculations are performed only at the Ce top sites since the top site has been known the most stable adsorption site for H_2S.[1] Sulfur on the top of dopants is restrained in *x* and *y* directions. Figure (a) and (b) show adsorbed S^* on the Ce top of CeO_2[(a)] and the Sm−O bridge of Sm-doped CeO_2[(b)], respectively. [(c)]Adsorbates strongly interact with the lattice oxygen of the Ce−O bridge site. [(d)]None means that no stable configuration is found.

	CeO_2			Sm-doped CeO_2		
	Ce top	Ce−O bridge[(c)]	O top	Sm top	Sm−O bridge[(c)]	O top
H_2S^*	−0.21	-		−0.22	-	
HS^*	−0.67	−1.61		None[(d)]	−2.58	
S^*	−0.70[(a)]	−2.58	−2.37	−0.88	−3.26[(b)]	−3.19

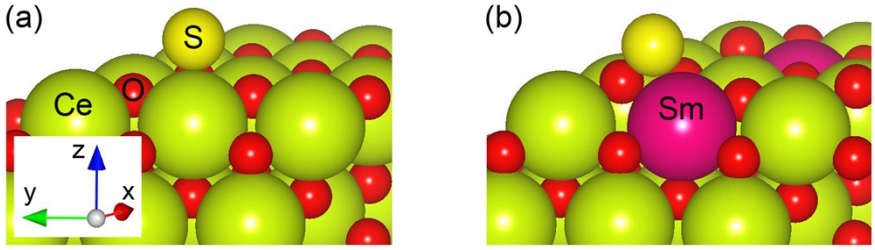

4. Total and projected density of state

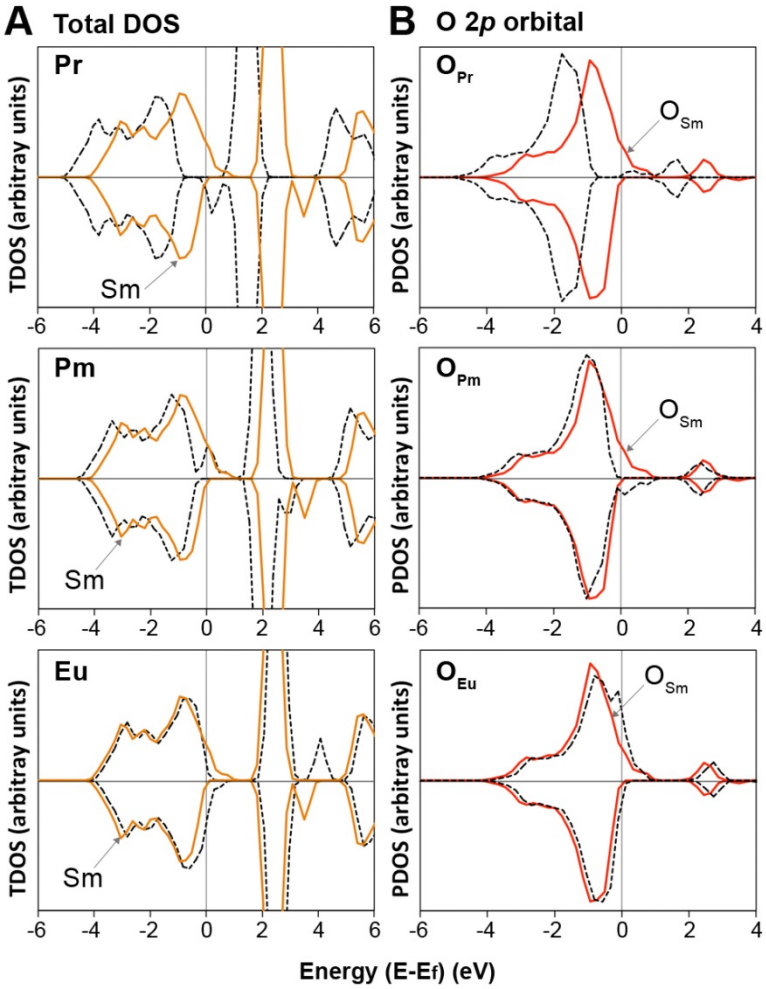

Figure S4. (A) TDOS of Pr-, Pm-, and Eu-doped CeO_2 (dashed lines) and Sm-doped CeO_2 (solid lines). (B) PDOS of surface O 2*p* states (four O atoms) of Pr-, Pm-, and Eu-doped CeO_2 (dashed lines), O_{Pr}, O_{Pm}, and O_{Eu}, respectively, and surface O 2*p* state (four O atoms) of Sm-doped CeO_2 (solid lines), O_{Sm}. Spin-up and -down are indicated by positive and negative values. The Fermi energy is referenced at 0 eV.

5. Diffusion of subsurface oxygen onto the surface

Subsurface oxygen atoms tend to diffuse onto the surfaces of stoichiometric CeO_2 and Sm-doped CeO_2 when two surface oxygen atoms are removed during the SO_2 formation and desorption. Sm doping enhances the stabilization of oxygen vacant Sm-doped CeO_2 by allowing a subsurface oxygen atom near Sm to diffuse onto the surface. In Figure S5, the diffusion distances of the first subsurface oxygen atoms marked by an arrow in stoichiometric CeO_2, Sm-doped CeO_2 (A), and Sm-doped CeO_2 (B) are 0.35, 0.44, and 1.07 Å, respectively. Without the surface oxygen vacancies, for example, SO_2* formed surfaces, the diffusion distances of the first

subsurface oxygen atoms on the three surface models are smaller and similar one another (0.24, 0.27, and 0.26 Å for stoichiometric CeO_2, Sm-doped CeO_2 (A), and Sm-doped CeO_2 (B), respectively).

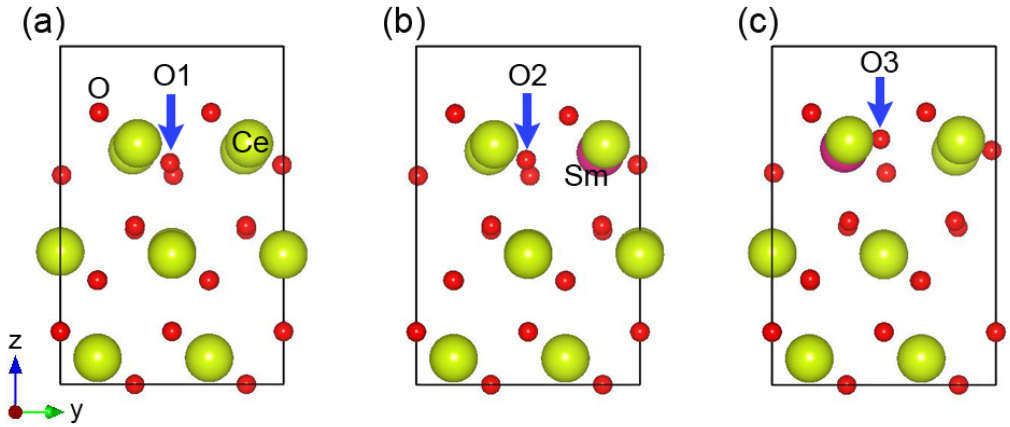

Figure S5. Location of subsurface oxygen atom in two surface oxygen vacant models of stoichiometric CeO_2 (a) and Sm-doped CeO_2 (b and c). (b) and (c) represent Sm-doped CeO_2 (A) and (B) in the main paper Figure 6, respectively.

References

(1) Marrocchelli, D.; Yildiz, B., First-Principles Assessment of H2S and H2O Reaction Mechanisms and the Subsequent Hydrogen Absorption on the CeO2(111) Surface. *Journal of Physical Chemistry C* **2012,** *116*, (3), 2411-2424.